

# Room temperature properties of microstructure and resistivity of alkaline earth – doped on lanthanide manganite

*Dwi Nanto*<sup>1,\*</sup>, *Desty Adella*<sup>2</sup>, *Arif Tjahjono*<sup>2</sup>, *Sitti Ahmiatri Saptari*<sup>2</sup>, *Sri Budiawanti*<sup>3</sup>, and *Agung Imaduddin*<sup>4</sup>

<sup>1</sup>Department of Physics Education, Faculty of Tarbiya and Teaching Science (FITK), UIN Syarif Hidayatullah, Jakarta 15412, Indonesia

<sup>2</sup>Department of Physics, Faculty of Science and Technology (FST), UIN Syarif Hidayatullah, Jakarta 15412, Indonesia

<sup>3</sup>Department of Physics Education, Faculty of Teacher Training and Education (FKIP), Universitas Sebelas Maret, Surakarta 57126, Indonesia

<sup>4</sup>Research Center for Advanced Material, National Research and Innovation Agency (BRIN), Puspiptek Area, South Tangerang, Banten 15314, Indonesia

**Abstract.** Microstructure of material has a strong relation with resistivity property. Here we report our interesting sample of  $\text{La}_{0.7}(\text{Sr}_{1-x}\text{Ba}_x)_{0.3}\text{MnO}_3$  ( $x = 0, 0.3, 0.6, \text{ and } 0.9$ ) material that has been synthesized by using sol-gel method successfully. All pattern of *X*-ray diffractometer (XRD) on the successful samples show that all samples are single phase confirmed without significant crystal disorder. The XRD pattern refinement yield that all samples formed R-3c space group with a rhombohedral structure. Although the substitution of  $\text{Ba}^{2+}$  to  $\text{Sr}^{2+}$  ions have significant difference in atomic radius; it does not change the crystal structure. However, the alkaline earth – doped on lanthanide manganite causes a change in lattice parameters which is followed by shifted of average crystal size, bond length, cell unit volume and bond angle at Mn-O-Mn. The microstructure results by means of scanning electron microscope (SEM) characterization shows that substitution of  $\text{Ba}^{2+}$  ions decrease the grain size and yield agglomeration. The relation on the microscopic result resistively confirmed by cryogenic magnetometer characterization in the concentration  $x = 0$  has minimum resistivity of  $1.28 \cdot 10^{-3} \Omega\text{m}$  and the maximum resistivity in the concentration  $x = 0.9$  is  $1.85 \cdot 10^{-1} \Omega\text{m}$ . The  $\text{Ba}^{2+}$  doped into  $\text{Sr}^{2+}$  in lanthanum manganite may cause a wider resistivity range.

**Keywords.** Manganite perovskite, sol-gel, grain size, resistivity

---

\* Corresponding author: [dwi.nanto@uinjkt.ac.id](mailto:dwi.nanto@uinjkt.ac.id)

## 1 Introduction

Research on manganite perovskite with general formula  $RE_{(1-x)}AE_xMnO_3$  ( $RE$  = rare-earth,  $AE$  =alkaline-earth such Ba, Ca or Sr) has been known that substitution manganites perovskite will imply to many unique physical processes such as magnetoresistance and magnetocaloric effect (MCE) [1, 2]. This material has potential to be applied in magnetic refrigeration, magnetic field sensors, spintronics, absorber materials, etc [3,4]. Substitution at  $RE$  site can cause Mn to have two electrons valence, those are  $Mn^{3+}$  and  $Mn^{4+}$  then cause double exchange (DE) interaction. DE is phenomena which transfer electron between  $Mn^{3+}$  and  $Mn^{4+}$  ions through  $O^{2-}$  anions [5].

Widyaiswari *et.al* [6] study of  $La_{0.67}Sr_{0.33}Mn_{1-x}Ni_xO_3$  to analyze the resistivity with cryogenic magnetometer. The result shows that material has insulator when temperature decreases from 300 K until 10 K. the resistivity of materials has increased along with increasing Ni substitution. The increase resistivity is accompanied with crystallite size getting smaller. Ngida *et.al* [7] reported alkaline earth on lanthanide manganite of  $La_xSr_{(1-x)}MnO_3$  ( $x=0.1, 0.3, 0.5$  and  $1.0$ ) and  $La_xCa_{(1-x)}MnO_3$  that synthesized using hydrothermal method. Those samples reveal that the electrical resistivity is dependent upon the grain size, microstructure, phase composition and porosity [7]. The sample investigation shows the sample are dense, compact and homogeneous microstructure with well-defined grain boundary and few amounts of pores. Their findings work has relatively smaller grain size and higher density as compared with other samples which sintered by conventional technique. Increasing the amount of Ca or Sr – doped in lanthanide manganite implies to the increasing intergranular porosity that caused the decrease in resistivity. Those facts describe that the porosity caused by the amount of doping element may imply to the density, microstructure and electrical properties of material.

Recently, Aydi *et.al* also reported the correlation between microstructure and electrical conductivity. Their evidence work shows that the conduction mechanism is strongly controlled by the grain boundary that confirmed by DC conductivity and impedance investigation [8]. They made  $La_{0.65}Ca_{0.25}Sr_{0.1}MnO_3$  by solgel method which morphological observed by means of scanning electron microscopy (SEM) that shows the grains have multi-shapes. According to DC investigation, they find that the curve of electrical conductivity in the whole temperature range shows a semiconducting character. Meanwhile they also investigated the electrical properties by using AC impedance method. They find that some electrical properties in undergone by the grain boundary which may come from grain capacitance, grain resistance, grain boundaries resistance grain boundaries charge, and constant phase elements.

Andreja *et.al* reporting a different method of preparing Sr-doped in manganite perovskite caused conductivity to increase with Sr-amount and temperature [9]. Their samples were  $La_{1-x}Sr_xMnO_3$  ( $x=0, 0.1, 0.2$  and  $0.3$ ) which conductivity of  $10^{-2}$ – $0.45 \Omega^{-1} \text{cm}^{-1}$  range. Pu *et. al.* reveal that the Sr doping level directly caused on the crystal structure parameters and affect the electrical transports property [10].

As the amount of Sr-doped content increase followed by increase gradually in  $T_p$ , transition temperature, that is metal-insulator (M-I) temperature. It also followed to the increase of peak temperature relating to temperature coefficient of resistivity (TCR). The fact of decreasing in resistivity causing an improve of TCR for the case.

In this work, we use sol-gel method to synthesize  $La_{0.7}(Sr_{1-x}Ba_x)_{0.3}MnO_3$  ( $x=0, 0.3, 0.6$  and  $0.9$ ). The crystal structure of the successful samples was investigated using X-ray Diffractometer (XRD), the surface morphology of the samples was examined using Scanning Electron Microscope (SEM) and to analysis resistivity of the samples by using cryogenic magnetometer.

## 2 Materials and method

La<sub>0.7</sub>(Sr<sub>(1-x)</sub>Ba<sub>x</sub>)<sub>0.3</sub>MnO<sub>3</sub> ( $x = 0, 0.3, 0.6$  and  $0.9$ ) was synthesized by the sol-gel method using some raw material from Merck Sigma - Aldrich chemical. The precursor material were La(NO<sub>3</sub>)<sub>3</sub>.6H<sub>2</sub>O, Sr(NO<sub>3</sub>)<sub>2</sub> and Ba(NO<sub>3</sub>)<sub>2</sub>.4H<sub>2</sub>O as RE-AE-site component, Mn(NO<sub>3</sub>)<sub>2</sub>.4H<sub>2</sub>O and C<sub>6</sub>H<sub>8</sub>O<sub>7</sub>.H<sub>2</sub>O under stoichiometric calculation. Those precursor were dissolved using distilled water, and La(NO<sub>3</sub>)<sub>3</sub>.6H<sub>2</sub>O was added using nitric acid (HNO<sub>3</sub>) until it get the clear solution and mix all the precursors. Then, the solution is put on magnetic hot plate to be stirred and heated to 80 °C. Ammonia solution is added until pH 7. After several time the viscous gel is formed. In order to eliminate the water content, then the sample will be dehydrated at 120 °C. The dried sample were then having pre-calcination at 650 °C for 6 hours and calcination at 1000 °C for 12 hours. The last step is sintering at 1200 °C for 6 hours which previously compacted at 10 ton. The successful sample were claimed by investigating crystal structure and phase purity which investigated by XRD under PanAnalytical Xpert Pro diffractometer with source of Cu  $\alpha$  ( $\lambda = 1,54056 \text{ \AA}$ ). The other physical properties characterization was continued to analyze the morphology and grain size using SEM FEI Quanta 650 and the resistivity was measured using Cryogenic Magnetometer.

## 3 Results and discussion

One may see on Fig. 1 that shows the experimental XRD pattern of all samples at room temperature. The result of Rietveld refinement of XRD pattern shows that all of sample have single phase without peak impurities. All the samples have rhombohedral structure with R-3c space group. The peak LSBMO shifted to the left when substitution of Ba increased. The fact strongly happened due to the ionic radius of Ba<sup>2+</sup> (1.61 Å) is larger than Sr<sup>2+</sup> (1.27 Å) [12]. Table 1 shows the results of XRD pattern refinement to analysis parameters from each sample.

Based on Table 1, substituting La<sup>2+</sup> in to Ba<sup>2+</sup> causes the crystal structure parameters increase such as volume unit cell, bond lengths but it decreases bond angles and electronic bandwidth ( $W$ ). Bandwidth can represent the double exchange interaction. If the  $W$  value decreases that means the electron on this material is more difficult to hopping shown in Fig. 2. Fontcuberta *et.al* reveal that structural distortion may affect to carrier mobility which controlled by the electronic bandwidth coming from the bending of the Mn-O-Mn bond [12].

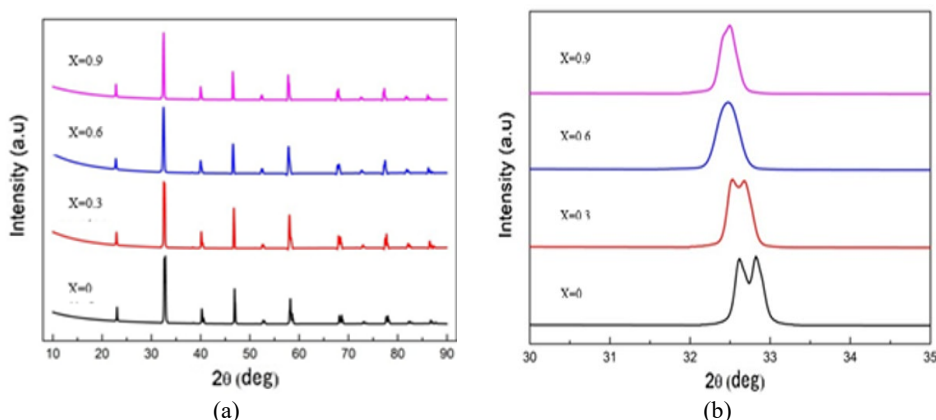


**Fig. 1.** (a) XRD pattern of La<sub>0.7</sub>(Sr<sub>(1-x)</sub>Ba<sub>x</sub>)<sub>0.3</sub>MnO<sub>3</sub> ( $x = 0, 0.3, 0.6$  and  $0.9$ ) samples. (b) the shifted XRD peak pattern of La<sub>0.7</sub>(Sr<sub>(1-x)</sub>Ba<sub>x</sub>)<sub>0.3</sub>MnO<sub>3</sub> ( $x = 0, 0.3, 0.6$  and  $0.9$ ) samples.

Their work claimed that the electronic bandwidth associated to an increase of the lattice distortion caused the decreasing of the localization length and imply to reduce the carrier mobility.

**Table 1.** Rietveld refinement result from XRD pattern measured for  $\text{La}_{0.7}(\text{Sr}_{1-x}\text{Ba}_x)_{0.3}\text{MnO}_3$  ( $x=0, 0.3, 0.6, \text{ and } 0.9$ ).

Parameter structural	$x = 0$	$x = 0.3$	$x = 0.6$	$x = 9$
$a(\text{\AA})$	5.4930	5.5060	5.5215	5.5539
$b(\text{\AA})$	5.4930	5.5060	5.5215	5.5539
$c(\text{\AA})$	13.3340	13.3600	13.4089	13.4560
$V(\text{\AA}^3)$	348.43	350.76	355.35	357.53
Average Crystallite size (nm)	69.59	61.43	48.16	65.56
Discrepancy factors				
Rwp (%)	6.32	7.97	9.23	8.82
Rp (%)	4.93	5.81	6.56	6.37
GoF	1.04	1.42	1.68	1.39
Bond lengths ( $\text{\AA}$ )				
$\langle \text{Mn} - \text{O} \rangle$	1.953	1.959	1.963	1.969
Bond angles ( $\text{\AA}$ )				
$\langle \text{Mn} - \text{O} - \text{Mn} \rangle$	167.371	166.545	166.358	165.789
Electronic Bandwidth (u.a)				
$W (10^{-2})$	9.54	9.44	9.37	9.26
Tolerance factor				
Goldschmidt	0.973	0.978	0.984	0.989

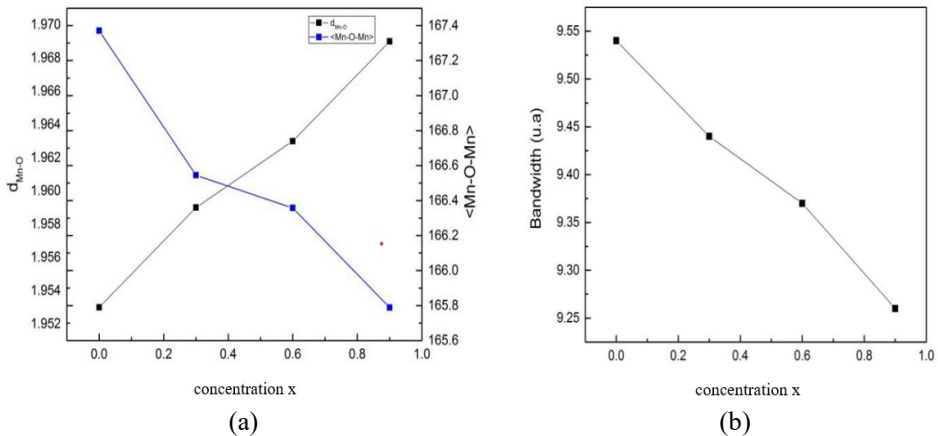
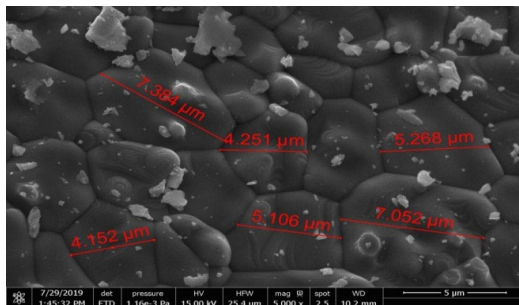
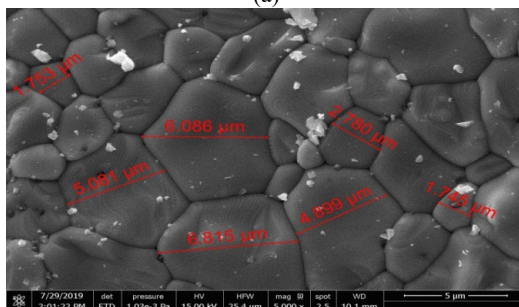


**Fig. 2.** Relation between (a) the bond length and bond angle, (b) electronic bandwidth with the concentration  $x$  of  $\text{La}_{0.7}(\text{Sr}_{1-x}\text{Ba}_x)_{0.3}\text{MnO}_3$  ( $x = 0, 0.3, 0.6$  and  $0.9$ ).

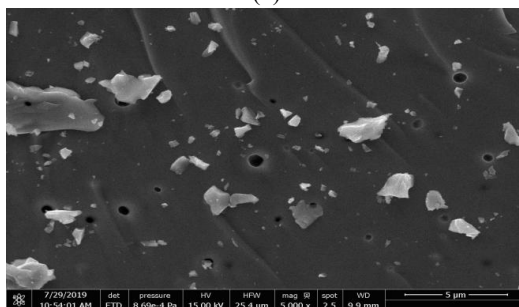
The surface morphology of the samples has been investigated using SEM shown in Fig. 3 according to the SEM result for sample  $x = 0$  has a larger grain size than  $x = 0.3$ . For samples  $x = 0.6$  and  $0.9$ , grain in both of samples cannot determine because of the agglomeration formed. According to Bhavani, Ba substitution cause agglomeration [13].



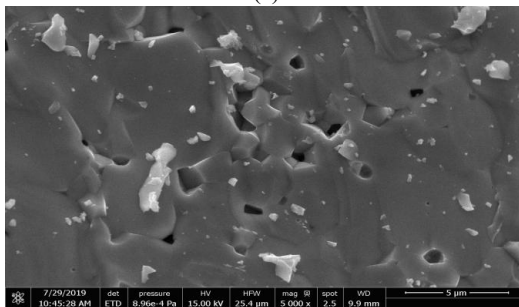
(a)



(b)



(c)



(d)

**Fig. 3.** SEM characterization of  $\text{La}_{0.7}(\text{Sr}_{1-x}\text{Ba}_x)_{0.3}\text{MnO}_3$  sample with a)  $x = 0$ , b)  $x = 0.3$ , c)  $x = 0.6$  and d)  $x = 0.9$ .

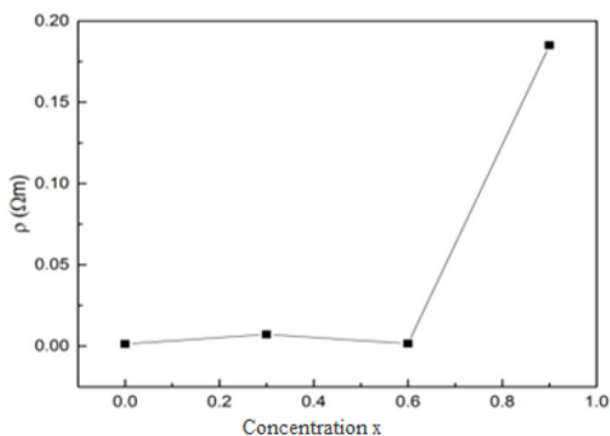


**Fig. 4.** The resistivity of  $\text{La}_{0.7}(\text{Sr}_{1-x}\text{Ba}_x)_{0.3}\text{MnO}_3$  ( $x = 0, 0.3, 0.6$  and  $0.9$ ) at room temperature.

Figure 4 shows the resistivity of  $\text{La}_{0.7}(\text{Sr}_{1-x}\text{Ba}_x)_{0.3}\text{MnO}_3$  ( $x = 0, 0.3, 0.6$  and  $0.9$ ). The sample with concentration  $x = 0.9$  has a maximum resistivity. According to Widyaiswari *et al.*[14] the increasing resistivity values are associated with increasingly difficult electron tunneling processes when the crystallite size decreases. In the previous XRD refinement data can be seen that the ability of double exchange decreases with increasing concentration  $x$ . the reducing ability of the DE affected by decreasing interactions between  $\text{Mn}^{3+}$  and  $\text{Mn}^{4+}$  ions, thus the electrons are getting more difficult to move. This condition causes the resistivity for  $x = 0.9$  reaches maximum. The  $\text{Sr}^{2+}$  and  $\text{Ba}^{2+}$  doped in lanthanum manganite may cause a wider resistivity range compared to Andreja *et.al* reported work [15].

## 4 Conclusion

We successfully synthesized  $\text{La}_{0.7}(\text{Sr}_{1-x}\text{Ba}_x)_{0.3}\text{MnO}_3$  ( $x = 0, 0.3, 0.6$  and  $0.9$ ) using sol-gel method. Refinement result of XRD pattern showed all samples in a single phase without significant impurities product and those samples possess rhombohedral structure with R-3c space group. The  $\text{Ba}^{2+}$  substitution into  $\text{Sr}^{2+}$  content causes a change in cell unit volume, average crystal size, lattice parameters, bond length and bond angle at Mn-O-Mn but does not change the crystal structure even though  $\text{Ba}^{2+}$  and  $\text{Sr}^{2+}$  ions have significant difference in atomic radius. Interestingly, it yields a wider resistivity range. The results of SEM characterization show that substitution of  $\text{Ba}^{2+}$  ions decrease the grain size and create agglomeration. The result of cryogenic magnetometer characterization in the concentration  $x = 0$  has minimum resistivity that  $1.28 \cdot 10^{-3} \Omega\text{m}$  and the maximum resistivity in the concentration  $x = 0.9$  is  $1.85 \cdot 10^{-1} \Omega\text{m}$  at room temperature.

## Acknowledgements

We acknowledge Juli Hartati, Ratna Isnanita Admi and Redho Aulia Putra for their invaluable help during laboratory work. This work is funded by PUSLITEPEN UIN Syarif Hidayatullah research grant of UN.01/KPA/223/2022.

## References

1. V. Dhokiya et al., *Mater. Chem. Phys.* **277**, 125430 (2022).
2. S. Choura-Maatar et al., *J. Mater. Sci.* **31**, 1634-1645 (2020).
3. K. P. Shinde, S. S. Pawar, P. M. Shirage, and S. H. Pawar, *Appl. Surf. Sci.* **258**, 7417-7420 (2012).
4. R. Pratama et al., *AIP Conf. Proc.* **1729**, 020028 (2016).
5. S. J. Youn and B. I. Min, *Phys. Rev.* **B 56**, 12046-12049 (1997).
6. W. Utami, K. Budhy, I. Agung, and S. Sitti Ahmiatri, *Spektra J. Fis. Apl.* **1**, 143-148 (2016).
7. R. E. A. Ngida, M. F. Zawrah, R. M. Khattab, and E. Heikal, *Ceram. Int.* **45**, 4894-4901 (2019).
8. S. Aydi et al., *Appl. Phys. A* **127**, 931 (2021).
9. A. Žužić, A. Ressler, A. Šantić, J. Macan, and A. Gajović, *J. Alloys. Compd.* **907**, 164456 (2022).
10. X. Pu et al., *J. Magn. Magn. Mater.* **560**, 169679 (2022).
11. S. M. Ramay, A. Mahmood, S. Atiq, and A. N. Al-Hazaa, *Int. J. Mod. Phys.* **B 30**, 1650020 (2016).
12. J. Fontcuberta, B. Martínez, A. Seffar, S. Piñol, J. L. García-Muñoz, and X. Obradors, *Phys. Rev. Lett.* **76**, 1122-1125 (1996).
13. A. G. Bhavani, W. Y. Kim, and J. S. Lee, *ACS Catal.* **3**, 1537-1544 (2013).
14. B. K. U. Widyaiswari, A. Imaduddin, and S. A. Saptari, *Spektra J. Fis. Apl.* **1**, 143-148 (2016).
15. A. R. A. Žužić, A. Šantić, J. Macan, and A. Gajović, *J. Alloys. Compd.* **907**, 164456 (2022).